ACS APPLIED MATERIALS & INTERFACES

RESEARCH ARTICLE

www.acsami.org

Tuning Porosity of Ti-MCM-41: Implication for Shape Selective Catalysis

Shengping Wang, Yun Shi, Xinbin Ma,* and Jinlong Gong*

Key Laboratory for Green Chemical Technology of Ministry of Education, School of Chemical Engineering and Technology, Tianjin University, Tianjin 300072, China

ABSTRACT: This paper describes a method to regulate porosity of Ti-containing mesoporous molecular sieves (Ti-MCM-41) by employing swelling agents that are hydrophobic in nature, such as dodecylamine, *n*-heptane, and sym-trimethylbenzene (TMB). Physicochemical properties of the samples were investigated using XRD, FT-IR, IR spectra of pyridine absorption, UV−vis, TEM, and N_2 adsorption−desorption techniques. Addition of favorable swelling agents leads to an increase in pore size accompanied by retaining the mesostructure with a certain decrease of structure ordering. Swelling agents also have significant impact on the integration of Ti into the silica framework, which further affect the formation of Lewis acid sites. *N*-heptane is the most favorable agent for pore expansion of Ti-MCM-41. The material with *n*-heptane/CTAB ratio of 1 exhibits the largest pore size of 48.3 Å, and mesopore volume of 1.266 cm^3/g and narrow pore-size distribution. We also demonstrated that shape-selective transesterification catalytic activity of Ti-MCM-41 was greatly enhanced because of pore expansion.

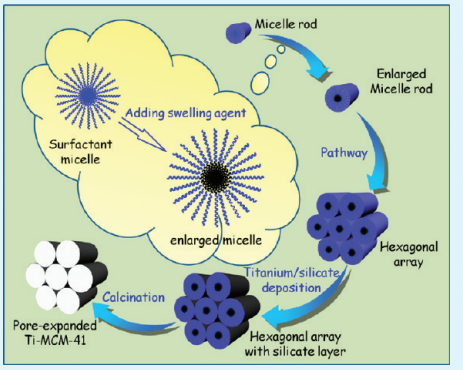

KEYWORDS: Ti-MCM-41, pore expansion, swelling agent, shape selectivity, organic carbonate

INTRODUCTION

Ordered mesoporous materials designated as M41S have aroused great interest since their invention in 1992.[1] These materials exhibit a number of desirable physical properties such as large surface area and pore volume, high thermal stability, and ease of surface modifications, which would combine the advantages of high loading of active components and enhanced mass transfer during catalytic reactions. Among these ordered mesoporous materials, MCM-41 molecular sieves, with a hexagonal array and uniform mesopore channels, is attractive in the fields of heterogeneous catalysis, adsorption, and separation.[2−7] Great efforts have been devoted to synthesis, modification of framework structures and compositions, particle morphology, and texture of MCM-41-based materials. Functionalized MCM-41 materials have been widely utilized in a number of shape-selective catalytic reactions, e.g., hydrodesulfurization,[8] isomerization,[9,10] dehydrocyclization,[11] and transesterification reaction.[12,13]

Regulation of pore size is a crucial aspect to attain high selectivity in heterogeneous catalysis, e.g., for those molecules that have small diffusion coefficiency in micropores. A number of methods (e.g., using long chain surfactants as templates, adding swelling agents as expanders, and hydrothermal postsynthesis treatment) have been developed for expanding the pore size of mesoporous materials.[14−17] Notably, addition of swelling agent has been proved to be an effective way for pore regulation. According to solubilization theory, hydrophobic additives can expand surfactant micelle effectively.[18,19] A variety of hydrophobes have been reported for pore size expansion, such as aromatic hydrocarbons,[20] long-chain alkanes,[21] long-chain alkylamines,[22,23] and mixed surfactants.[24] However, resultant large pore size is occasionally accompanied with the structural disordering (i.e., the hexagonal structure of channels would be disarranged). Thus, the selection of suitable organic additives is fairly important for pore expansion based on textural stability.

A number of investigations have been reported regarding expansion of porosity of MCM-41 molecule sieves,[5,14−17,25,26] few of which, however, concern heteroatom-substituted MCM-41 mesoporous sieves. Accordingly, this paper describes a strategy to regulate the porosity properties of Ti-containing mesoporous molecular sieves (Ti-MCM-41) by utilizing organic swelling agents in synthesis procedure, and discusses how the addition of swelling agents would change physicochemical properties of Ti-MCM-41. The pore-expanded Ti-MCM-41 materials were prepared under a microwave irradiation condition to obtain uniform mesoporous texture in a shorter crystallization period. We chose several organic agents with different hydrophobicity as swelling agents (SA), including dodecylamine, *n*-heptane, and trimethylbenzene (TMB) to tune the porosity of the prepared Ti-MCM-41. Structural and physicochemical properties of these materials were examined by a number of characterization tools including small-angle X-ray powder diffraction (SAXRD), Fourier transform infrared (FT-IR) spectroscopy, N_2 adsorption−desorption, transmission electron micrograph (TEM), and diffuse reflectance UV−visible (DRUV−vis) spectroscopy. We employed transesterification of dimethyl oxalate (DMO) with phenol as a probe reaction to test the shape-selective functionality of these catalytic materials.

Received: March 27, 2011
Accepted: May 24, 2011
Published: May 24, 2011

EXPERIMENTAL SECTION

Materials. Tetraethyoxysilane (TEOS), tetrabutyl titanate (TBOT), cetyltrimethylammonium bromide (CTAB), sodium hydroxide (NaOH), isopropyl alcohol (*i*-PrOH), dodecylamine, *n*-heptane, and TMB were all purchased from Kermel Fine Chemical Corporation (Tianjin, China). Dimethyl oxalate and phenol were obtained from Tianjin NO. One Chemical Reagent Factory (Tianjin, China). All of these chemicals are analytical reagent-grade. Acetonitrile is HPLC grade acquired from Fisher Scientific Corporation (NJ, USA).

Synthesis of Ti-MCM-41. Pore-expanded titanium-containing mesoporous catalysts were directly synthesized under a microwave irradiation condition, using organic water-insoluble agent as a pore expander. Detailed synthetic procedure was carried out as follows: CTAB (3.64 g) and a certain amount of SA were dissolved in 90 mL of deionized water under vigorous stirring at 313 K, and then TEOS (15.32 g) was added dropwise to the surfactant solution followed by an adjustment of pH value to 11.0 through gradual addition of a NaOH solution. After 10 min, TBOT (0.50 g) dissolved in *i*-PrOH was dropped into the mixture. The stirring was maintained for 40 min for the sufficient hydrolysis of TEOS and TBOT. The pH value of mixed solution adjusted by the NaOH solution was between 10.5 and 11.0. Molar composition of final gel was 1:7.35:0.147:1.5:500:7.35 CTAB:TEOS:TBOT:NaOH:H_2O:*i*-PrOH. The SA/CTAB molar ratio was 1, except for *n*-heptane which was varied from 0.5 to 2. The resultant suspension was transferred into Teflon vessels and heated via nonpulsed microwave irradiation in a Multiwave 3000 microwave reaction system (Anton Paar) that is equipped with an 8-rotor tray. Combined with a temperature sensor, a pressure sensor, and an adjustable power output (maximum 1200 W), the microwave system provides an efficient way for rapid and uniform heating. Crystallization was performed in the temperature controlled mode where the temperature was ramped for 5 min and hold 393 K for 40 min. The maximum pressure increase rate was set to be 0.3 bar s^{-1}; and the maximum pressure in the reaction vessels was programmed not to exceed 2 MPa. After cooling to room temperature, the solid products were isolated by filtering, washed with deionized water, and dried in air at 373 K for 12 h. Subsequently, the dried samples were calcined at 823 K for 6 h in air with a heating rate of 2 K/min.

Characterization of Materials. SAXRD measurements were performed on a Rigaku D/max-2500 diffractometer using graphite filtered Cu Kα radiation (λ = 0.154056 nm) at 40 kV and 100 mA. Diffraction data were recorded at an interval of 0.02° and a scanning speed of 1° min^{-1} in the range of 1−10°.

TEM images of the samples were obtained on a Tecnai G2 F20 (FEI) transmission electron microscope at 200 kV.

N_2 adsorption−desorption isotherms were obtained at 77 K using a Tristar 3000 surface area and porosity analyzer (Micrometritics). Before measurements, the samples were outgassed at 573 K for 3 h in a degas port of the analyzer. Surface areas were calculated by the Brunauer−Emmet-Teller (BET) method and the pore size distribution was determined via the Barrett−Joyner−Halenda (BJH) method based on the Kelvin equation.[27]

FT-IR spectra of samples were recorded in the range of 400 to 4000 cm^{-1} on a Nicolet 6700 spectrometer (Nicolet) with a KBr pellet. Acidity of catalysts was analyzed by FTIR measurement of adsorbed pyridine using the same IR spectrometer with a 4 cm^{-1} resolution. The samples were pressed into a self-supporting wafer followed by evacuation at 623 K for 0.5 h. After cooled down to 333 K, pyridine was adsorbed on the samples until saturation. Subsequently, the samples were outgassed 0.5 h at 333 K and the spectra were recorded.

Coordination environment of Ti species was determined by DRUV−vis spectroscopy. The measurement was performed at room temperature using a UV-3600 spectrometer (Shimazu) in the wavelength range of 190−700 nm.

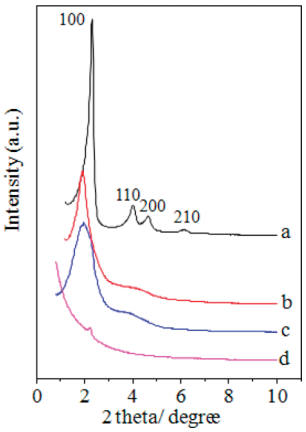

Figure 1. XRD patterns of Ti-MCM-41 samples synthesized using different swelling agents: (a) no swelling agent, (b) TMB, (c) *n*-heptane, and (d) dodecylamine.

Catalytic Reaction. Transesterification reaction of DMO with phenol was conducted in a three-necked round bottomed flask (125 mL) equipped with a thermometer, a condenser, and a magnetic stirrer under refluxing condition at atmospheric pressure with Ti-MCM-41 as catalyst. The condenser consisted of a distillation column kept at 353 K by flowing recycled hot water in order to remove produced methanol to push the reaction toward the desired direction. In a typical experiment, DMO and phenol with a molar ratio of 1:3 and an appropriate amount of Ti-MCM-41 were added into a batch reactor. Nitrogen gas was then flowed at 30 sccm for 10 min to purge the air from the reaction system. The reaction temperature was kept at 453 K, and the reaction time was 2 h. Quantitative analysis of reaction products was performed on an HP1100 series high-performance liquid chromatography (Agilent Technologies) equipped with a quaternary gradient pump, an online degasser and an ultraviolet visible detector (VWD). A ZORBAX Eclipse XDB-C18 column (150 mm × 4.6 mm, 5 μm, Agilent Technologies) was used for the liquid-chromatographic analysis of the products. The separation was achieved under a step-gradient elution condition with a mixed mobile phase consisting of water and acetonitrile and the UV detection at 254 nm at atmospheric temperature.

RESULTS AND DISCUSSION

Influence of Swelling Agents on Structural Property of Ti-MCM-41. Figure 1 shows small-angle XRD patterns of Ti-containing mesoporous catalysts prepared using different swelling agents. In the absence of swelling agent, the sample exhibits four well-defined peaks including a main reflection peak corresponding to the (100) plane at a small angle (2θ = 2−3°) and other three weak peaks around 3−7° indexed with (110), (200), (210) facets. It represents a typical hexagonal channel texture of MCM-41.[1] Upon addition of swelling agents except for dodecylamine, the materials remain their characteristic long-ranged structure as evidenced by the reflection peak representing the (100) plane. However, this peak is weaker and wider in the presence of swelling agents, and the other three peaks become indistinct. It indicates that swelling agents can slightly disorder the hexagonal arrangement of Ti-MCM-41 materials. Notably, the sample prepared with dodecylamine shows a very small and ambiguous peak attributed to the (100) facet, implying that the hexagonal channel is destroyed significantly.

FTIR spectra reveal the formation of Si−O−Ti linkages. FTIR spectra of samples prepared in the presence of different

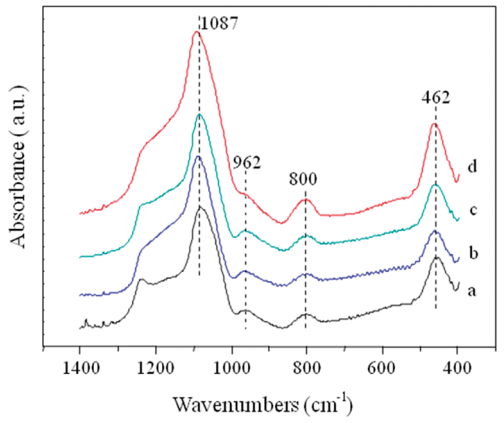

Figure 2. FT-IR spectra of Ti-MCM-41 samples synthesized using different swelling agents: (a) no swelling agent, (b) *n*-heptane, (c) TMB, and (d) dodecylamine.

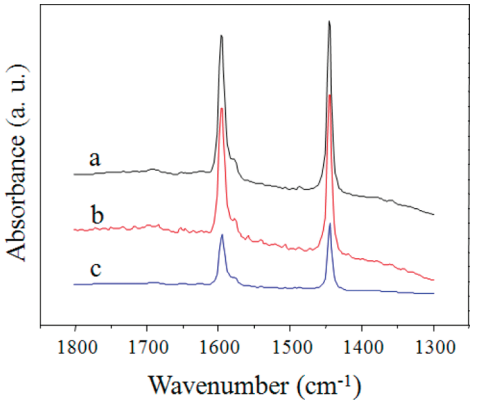

Figure 3. FT-IR spectra of pyridine adsorbed on Ti-MCM-41 samples synthesized using different swelling agents: (a) *n*-heptane, (b) TMB, and (c) dodecylamine.

swelling agents (Figure 2b–d) are similar to that of Ti-MCM-41 (Figure 2a). The strong absorbances at 1087 cm^{-1} and 800 cm^{-1} are assigned to asymmetric and symmetric stretching vibrations of Si–O–Si, respectively.[7,28] The band ~462 cm^{-1} is corresponded to bending vibration of Si–O–Si bonds. The band ~962 cm^{-1} is clearly detected for all the samples, which is associated with Si–O–Ti bonds.[29−31] These results demonstrate that swelling agents have little influence on the structure of the framework of MCM-41. Furthermore, the absorbance represents the amount of corresponding linkage. For the samples prepared in the presence of *n*-heptane and TMB, the absorbances standing for both Si–O–Si and Si–O–Ti linkages are almost as strong as those of Ti-MCM-41 prepared in the absence of swelling agent. However, there are remarkable changes in IR absorption of the sample prepared with dodecylamine. Intensity of the bands related with Si–O–Si bonds, such as 1087 cm^{-1}, 800 cm^{-1}, and 462 cm^{-1}, increases greatly. In contrast, the 962 cm^{-1} band associated with Si–O–Ti linkages decreases. It suggests that swelling agents significantly impact on the incorporation of titanium into the silica framework.

Si–O–Ti bonds can form acid sites on the surfaces of Ti-MCM-41. As a base molecule, pyridine can react with acid sites on surface of catalysts, and thus is often used as a probe molecule

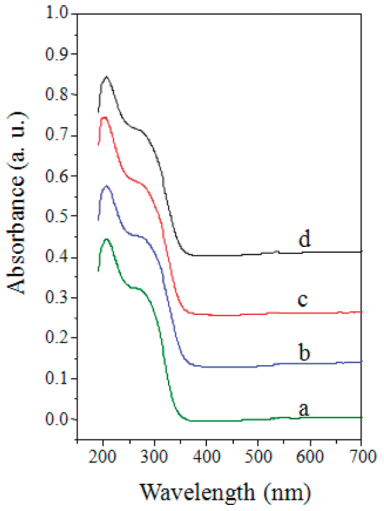

Figure 4. UV–visible diffuse reflectance spectra of Ti-MCM-41 samples synthesized using different swelling agents: (a) no swelling agent, (b) *n*-heptane, (c) TMB, and (d) dodecylamine.

for qualitative and quantitative determination of the types of acid sites.[32,33] Figure 3 shows FTIR spectra of adsorbed pyridine on Ti-MCM-41 samples prepared in the presence of swelling agents. The band appearing ~1445 cm^{-1} is attributed to pyridine molecules connected to silanol groups with weak hydrogen bonding and coordinated to Lewis acid sites. The band at ~1540 cm^{-1} is assigned to pyridine adsorption on Brönsted acid sites. It is apparent that the band at 1445 cm^{-1} is present for all the samples, whereas the band at 1540 cm^{-1} is absent, indicating that acid sites on the surface are dominantly Lewis acid sites. Another band appearing at 1596 cm^{-1} can be attributed to hydrogen-bonded pyridine. It has been reported that the hydroxyls are not capable to protonate pyridine,[34] thus it is very likely that pyridine molecules form hydrogen bonds with the sillanol group presented in the structure. We notice a weaker absorption band in spectra for the sample prepared with dodecylamine, suggesting a lack of acid sites on the surfaces. Addition of dodecylamine can lead to a great decrease in intensity of Si–O–Ti linkages, which is primarily responsible for the small amount of acid sites measured by pyridine adsorption.

DRUV–vis spectroscopy is a sensitive probe to distinguish exterior- and inner-framework Ti species, and the variation observed on the peak could reflect the qualitative and quantitative changes of titanium in zeolite.[35−37] DRUV–vis spectra (Figure 4) demonstrate that swelling agents do not significantly influence the coordination environment of titanium in the sample since the absorption bands all looks similar. These samples all show a strong absorption band centered at 210 nm, which is associated with the isolated tetrahedral titanium species, and is arising from the electronic transfer between titanium and oxygen in the framework.[38] Another weak band ~260–280 nm is due to small amounts of polymerized Ti species in a high coordination (such as penta or hexahedral coordination).[39] The lack of absorption band at ~330 nm implies the absence of octahedral anatase-like titania, which further indicates that all titanium integrated into the silica framework.[39,40]

We also measured porosity of the materials by N_2 adsorption. Figure 5A illustrates N_2 adsorption–desorption isotherms from samples prepared with different swelling agents. All samples give

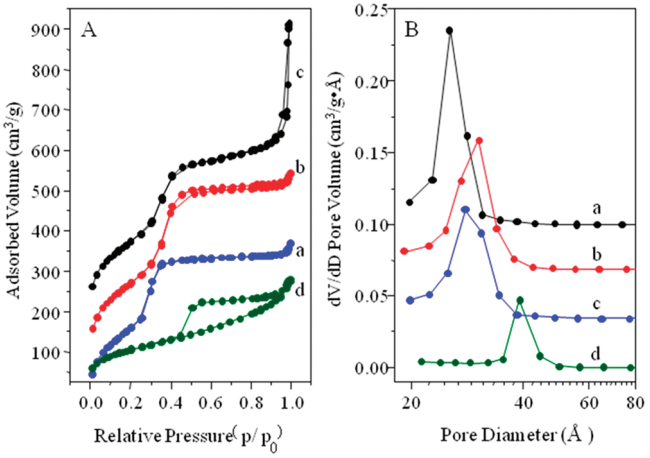

Figure 5. (A) Nitrogen adsorption−desorption isotherms and (B) pore size distribution curves of the Ti-MCM-41 samples synthesized using different swelling agents: (a) no swelling agent, (b) TMB, (c) *n*-heptane, and (d) dodecylamine.

Table 1. Pore Structure Parameters of Ti-MCM-41 samples prepared with different swelling agents

swelling agent[a]	S_{BET} (m^2/g)	V_{BJH} (cm^3/g)	D_{BJH} (Å)
	887	0.830	28.6
dodecylamine	380	0.465	45.1
n-heptane	844	1.266	48.3
TMB	883	0.866	30.5

[a] SA/CTAB molar ratio is 1.

typical irreversible type IV adsorption isotherms. The isotherm of unmodified Ti-MCM-41 (Figure 5A(a)) includes a linear increase of adsorbed volume at low relative pressure followed by a steep increase in the adsorbed volume of N_2 and finally by a slight increase at high relative pressure. The isotherms of samples prepared with TMB and *n*-heptane follow the similar trend. As the relative pressure increases, the isotherms exhibit a sharp inflection in the p/p_0 range from 0.25 to 0.45, which is a characteristic of capillary condensation inside mesopores. The p/p_0 position of the inflection points is clearly related to a diameter in the mesopore range, and the sharpness of these steps indicates the uniformity of mesopore size distribution. It is obvious that the samples prepared with swelling agents present inflection with a slight shift toward higher relative pressure, indicating the pore-expanded effect of swelling agents. The sample prepared by *n*-heptane yields an isotherm with a sharp inflection at approximate saturation vapor pressure, which is due to a capillary condensation in large cavities. We notice that the isotherm of sample prepared with dodecylamine (Figure 5A(d)) is somewhat difference as it presents no inflection step in mid relative pressure range but a big hysteresis loop referring to numbers of large pores of irregular shape and size.

Pore size distribution of the samples prepared with addition of swelling agents was investigated and the results are shown in Figure 5B. The unmodified Ti-MCM-41 possesses a fairly narrow pore size distribution with a most probable diameter of 27.5 Å. For the samples prepared in the presence of swelling agents, both fwhm and the most probable diameter are increased greatly, indicating the expansion of pore sizes. Table 1 summarizes structural parameters

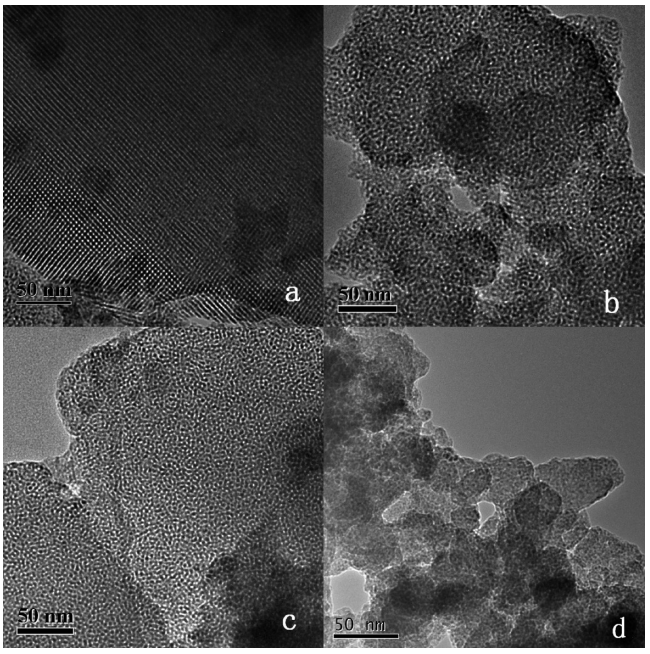

Figure 6. TEM images of Ti-MCM-41 samples synthesized using different swelling agents: (a) no swelling agent, (b) *n*-heptane, (c) TMB, and (d) dodecylamine.

calculated from N_2 adsorption−desorption isotherms. Average pore diameter (D_{BJH}) and the pore volume (V_{BJH}) increase upon the addition of swelling agents. Although the sample prepared with dodecylamine exhibits a significant increase of D_{BJH}, both the specific surface area (S_{BET}) and V_{BJH} decrease. Coupled with XRD results, for the samples prepared with dodecylamine, the typical structure of Ti-MCM-41 is changed leading to a texture of amorphous titanium silicon oxides. It may be because carbon chain of decylamine is so long that when dodecylamine molecule enters the center of surfactant micelles, the intermicellar equilibrium would be broken.[41] Thus, the channel structure is destroyed greatly. Additionally, the other two additives have expanded pore size on the base of maintaining the high surface area. Specifically, *n*-heptane yields optimal pore-expanding ability, giving the largest average pore size (48.3 Å) and pore volume (1.266 cm^3/g). Indeed, the capability of pore expansion of swelling agents would be associated with their hydrophobicity.[42] For instance, *n*-heptane molecule is more hydrophobic compared to TMB; thereby more *n*-heptane molecules could join into surfactant micelles. Consequently, *n*-heptane behaved more effectively for pore size expansion.

Figure 6 shows transmission electron micrographs of obtained Ti-MCM-41 samples. Without porosity regulation, bare Ti-MCM-41 sample exhibits straight, parallel and uniform channel arrangement with electronic beam passing through both parallel and vertical direction to the axis of channels (Figure 6a). Furthermore, these channels do not connected with each other. Upon addition of swelling agent, the samples prepared with TMB and *n*-heptane show disordered wormhole-like pore structures, which is a characteristic for mesostructure.[43] This randomly interrupted arrangement of pores is attributed to the presence of cavities that eventually interconnected through necks.[44] However, the sample prepared with dodecylamine shows an amorphous structure similar to silicon dioxide.

Influence of Quantity of Swelling Agent on Structure of Ti-MCM-41. We have found that *n*-heptane is an excellent swelling

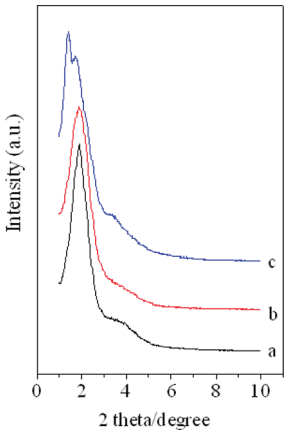

Figure 7. XRD patterns of Ti-MCM-41 samples synthesized in the presence of *n*-heptane: (a) SA/CTAB = 0.5, (b) SA/CTAB = 1, and (c) SA/CTAB = 2.

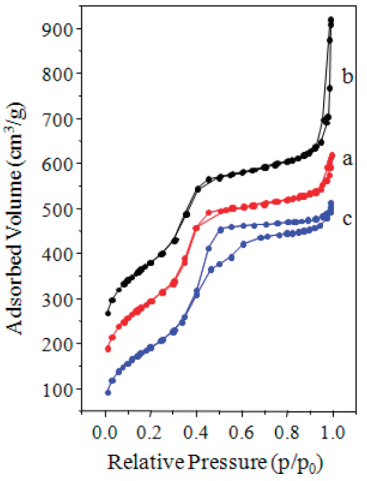

Figure 8. Nitrogen adsorption−desorption isotherms of the Ti-MCM-41 samples synthesized in the presence of *n*-heptane: (a) SA/CTAB = 0.5, (b) SA/CTAB = 1, and (c) SA/CTAB = 2.

agent that could expand the pore size of Ti-containing mesoporous materials effectively, simultaneously maintaining the characteristics of high specific surface area and large pore volume. In order to further understand the swelling process, we have examined the influence of quantity of swelling agent (i.e., *n*-heptane) on the structure of materials. Addition of swelling agent should be limited within a certain range; proper concentration of swelling agent is beneficial to pore expansion, whereas excessive utilization would disturb the stability of surfactant micelles.[14] According to this rule, we chose molar ratios of SA/CTAB of 0.5, 1, and 2.

XRD patterns of Ti-MCM-41 samples prepared with different SA/CTAB molar ratios are shown in Figure 7. As the ratio of SA/CTAB increases from 0.5 to 1, the main peak around 2° becomes blunt and the fwhm increases accordingly. Upon further increasing molar ratio of SA/CTAB to 2, the main reflection peak is split, suggesting the disarrangement of channels. These results provide evidence that increasing amount of added swelling agent could disorganize the order structure of Ti-MCM-41 samples, even destroy the regular channel.

FTIR spectra of samples prepared in the presence of *n*-heptane with different SA/CTAB molar ratio has been carried out (not exhibited). The *n*-heptane/CATB ratio has little effect on intermolecular structure of the samples since nearly the same infrared absorption bands at 1087, 800, 462, and 962 cm^{-1} are observed. Additionally, effect of added amounts of *n*-heptane on exterior- and inner-framework Ti species of Ti-MCM-41 samples was also investigated employing DRUV−vis. The results indicate that most of the Ti species are isolated and in tetrahedral coordination, coexisting with some polymerized higher coordinated sites. No bulk TiO_2 structure was formed in all the Ti-MCM-41 samples.

Because swelling agents have different pore-expanding efficiency, the influence of quantity of swelling agent on porosity is another important aspect we should address. The tested samples all exhibit type IV adsorption isotherms with a sharp inflection at p/p_0 around 0.35 as a characteristic for M41S mesoporous structure, and an extra inflection at p/p_0 ~0.9 (Figure 8). The adsorption at approximate saturation vapor pressure is ascribed to the filling of the textural mesoporosity, as a result from the intergrowth or aggregation of nanoparticles.[45,46] With increasing amount of additive *n*-heptane, the number of secondary porosity increases. Particularly, the sample with a n-heptane/CTAB ratio of 2 yields isotherms with an obvious hysteresis loop at high relative pressure, referring to a considerable amount of secondary mesopores consisting of large cavities interconnected through the neck.[47] Structural parameters associated with porosity of the samples are listed in Table 2. An appropriate amount of *n*-heptane (e.g., *n*-heptane/CTAB ratio of 1) is beneficial for expanding the pore size of Ti-MCM-41. As the amount of swelling agent increase, the stability of surfactant micelle would be weakened, leading to a rearrangement of channels (e.g., a collapse of the structure). Therefore, excessive addition of swelling agent would negatively affects the increment of both pore size and specific surface area.

Table 2. Pore Structure Parameters of Ti-MCM-41 Samples Prepared in the Presence of *n*-Heptane

n-heptane/CTAB	S_{BET} (m^2/g)	V_{BJH} (cm^3/g)	D_{BJH} (Å)
0.5	824	0.918	35.4
1	844	1.266	48.3
2	781	0.875	33.4

Catalytic Activities of Pore-Expanded Ti-MCM-41. The unique structure and ordered channels of Ti-MCM-41 molecular sieves are responsible for a number of shape-selective heterogeneous reactions.[9,10] Subsequently, we have tested catalytic, shape-selective functionality of our Ti-MCM-41 materials with modified porosity by using transesterification of DMO with phenol as a probe reaction. The transesterification of DMO with phenol is considered as a promising green rout for diphenyl oxalate (DPO) synthesis, which is an important precursor for production of polycarbonates.[48] In this route, DPO is synthesized via two steps, namely the transesterification of DMO with phenol into methyl phenyl oxalate (MPO) and the disproportionation reaction of MPO to DPO. It has been reported that the molecular sizes of DMO (X = 6.4 Å, Y = 5.1 Å), phenol (X = 7.1 Å, Y = 4.9 Å, Z = 2.5 Å), MPO (X =8.4 Å, Y = 6.3 Å, Z = 5.6 Å), and DPO (X = 9.9 Å, Y = 5.7 Å, Z = 4.6 Å) are all relatively large.[49] Thus, the porosity of catalytic materials is a crucial factor that influences the selectivity of this reaction. Indeed, it has been shown previously that the catalytic activity of microporous material TS-1

Table 3. Activities of Catalysts for the Transesterification of Dimethyl Oxalate with Phenol

swelling agents	SA/CTAB	conversion (%)	yield (%)		selectivity (%)	
			DPO	MPO	DPO	MPO
		63.3	14.1	49.2	22.3	77.7
dodecylamine	1	57.3	10.8	46.5	18.9	81.1
TMB	1	67.4	16.4	51.0	24.3	75.7
n-heptane	0.5	70.1	17.1	52.9	24.5	75.5
n-heptane	1	71.3	19.0	52.3	26.6	73.4
n-heptane	2	69.1	17.3	51.8	25.0	75.0

is limited by the small channel diameters.[50] Therefore, the unique ordered mesoporous texture with desirable channel size would be beneficial for the diffusion of DMO and phenol and targeted products.[51]

Table 3 summarizes the results of the transesterification reaction on a series of pore expanded Ti-MCM-41 materials. All the samples are considerably active for the reaction. As expected, the samples prepared in the presence of TMB and *n*-heptane are more active than unmodified Ti-MCM-41. It is apparent that pore expansion is favorable to improve the catalytic performance for the two-step transesterification of DMO and phenol, particularly the disproportionation of MPO to DPO. Interestingly, the sample prepared in the presence of dodecylamine is not as favorable as other catalysts in terms of activity and selectivity, although it possesses the large average pore size. This is because the hexagonal ordered structure has been destroyed along with a drastical decrease of specific surface area, and the framework of titanium is also reduced greatly, accompanied by a reduced number of acid sites on surfaces of the sample.

We note that the catalyst treated with *n*-heptane exhibits favorable activities for the transesterification of DMO and phenol to DPO, consistent with its porosity properties. Owing to its well-ordered structure with large pore size and high surface area, the sample with *n*-heptane/CTAB of 1 yields the most favorable catalytic performance.

CONCLUSIONS

We have made successful attempts to tune porosity property of Ti-containing mesoporous molecular sieves synthesized under microwave irradiation condition using organic swelling agent, such as TMB, *n*-heptane, and dodecylamine. N_2 adsorption−desorption analysis, XRD spectra and TEM images indicate that the addition of suitable swelling agents increase the pore size significantly, accompanying with maintaining the mesostructure, although it has some little structural disordering. Swelling agents also have different impacts on the coordination of Ti inside the silica framework and the consequent formation of Lewis acid sites on surface of catalysts. Furthermore, *n*-heptane is an optimal swelling agent considering its efficiency regarding expansion pore size and volume. With a molar ratio of *n*-heptane/CTAB of 1, the materials maintained an ordered M41S structure and exhibited the largest average pore size (48.3 Å) and volume (1.266 cm^3/g) among the prepared Ti-containing materials. We have also showed evidence indicating these MCM-41 materials with tunable porosity can be beneficial for the shape-selective reactions, using transesterification of dimethyl oxalate with phenol as a probe reaction. These findings can be extended to relevant studies regarding tuning porosity of other molecular sieves and their shape-selective catalytic functionality.

AUTHOR INFORMATION

Corresponding Author

*E-mail: jlgong@tju.edu.cn (J.L.G.); xbma@tju.edu.cn (X.B.M.). Fax: +86-22-87401818.

ACKNOWLEDGMENT

Financial support from Natural Science Foundation of China (20506018, 21006068), the Program of Introducing Talents of Discipline to Universities (B06006), the National Key Project for the 11th Five Year Plan (2006BAE02B00), and the Program for New Century Excellent Talents in University is gratefully acknowledged.

REFERENCES

(1) Beck, J. S.; Vartuli, J. C.; Roth, W. J.; Leonowicz, M. E.; Kresge, C. T.; Schmitt, K. D.; Chu, C. T. W.; Olson, D. H.; Sheppard, E. W. *J. Am. Chem. Soc.* **1992**, *114*, 10834.
(2) Tatsumi, T.; Koyano, K. A.; Igarashi, N. *Chem. Commun.* **1998**, 325.
(3) Selvam, P.; Bhatia, S. K.; Sonwane, C. G. *Ind. Eng. Chem. Res.* **2001**, *40*, 3237.
(4) Qiao, S. Z.; Bhatia, S. K.; Nicholson, D. *Langmuir* **2004**, *20*, 389.
(5) Reynhardt, J. P. K.; Yang, Y.; Sayari, A.; Alper, H. *Adv. Funct. Mater.* **2005**, *15*, 1641.
(6) Sayari, A. *Chem. Mater.* **1996**, *8*, 1840.
(7) Kong, Y.; Zhu, H. Y.; Yang, G.; Guo, X. F.; Hou, W. H.; Yan, Q. J.; Gu, M.; Hu, C. *Adv. Funct. Mater.* **2004**, *14*, 816.
(8) Herrera, J. M.; Reyes, J.; Roquero, P.; Klimova, T. *Microporous Mesoporous Mater.* **2005**, *83*, 283.
(9) Silva, T. N.; Lopes, J. M.; Ribeiro, F. R.; Carrott, M. R.; Galacho, P. C.; Sousa, M. J.; Carrott, P. *React. Kinet. Catal. Lett.* **2002**, *77*, 83.
(10) Zou, J. J.; Zhang, M. Y.; Zhu, B.; Wang, L.; Zhang, X. W.; Mi, Z. T. *Catal. Lett.* **2008**, *124*, 139.
(11) Ciuparu, D.; Chen, Y.; Lim, S.; Haller, G. L.; Pfefferle, L. *J. Phys. Chem. B* **2003**, *108*, 503.
(12) Guerrero, V. V.; Shantz, D. F. *Ind. Eng. Chem. Res.* **2009**, *48*, 10375.
(13) Jimenez-Morales, I.; Santamaria-Gonzalez, J.; Maireles-Torres, P.; Jimenez-Lopez, A. *Appl. Catal., A* **2010**, *379*, 61.
(14) Kruk, M.; Jaroniec, M.; Sayari, A. *Microporous Mesoporous Mater.* **2000**, *35*−*36*, 545.
(15) Lin, H.-P.; Mou, C.-Y. *Microporous Mesoporous Mater.* **2002**, *55*, 69.
(16) Di, Y.; Meng, X.; Li, S.; Xiao, F.-S. *Microporous Mesoporous Mater.* **2005**, *82*, 121.
(17) Kruk, M.; Jaroniec, M.; Sayari, A. *Microporous Mesoporous Mater.* **1999**, *27*, 217.
(18) Kresge, C. T.; Leonowicz, M. E.; Roth, W. J.; Vartuli, J. C.; Beck, J. S. *Nature* **1992**, *359*, 710.
(19) Kruk, M.; Jaroniec, M.; Sayari, A. *J. Phys. Chem. B* **1999**, *103*, 4590.
(20) Kim, M. J.; Ryoo, R. *Chem. Mater.* **1999**, *11*, 487.
(21) Ulagappan, N.; Rao, C. N. R. *Chem. Commun.* **1996**, 2759.
(22) Sayari, A.; Hamoudi, S.; Yang, Y. *Chem. Mater.* **2004**, *17*, 212.
(23) Sayari, A.; Yang, Y.; Kruk, M.; Jaroniec, M. *J. Phys. Chem. B* **1999**, *103*, 3651.
(24) Widenmeyer, M.; Anwander, R. *Chem. Mater.* **2002**, *14*, 1827.
(25) Sayari, A.; Yang, Y. *J. Phys. Chem. B* **2000**, *104*, 4835.
(26) Mehn, D.; Konya, Z.; Halasz, J.; Nagy, J. B.; Rac, B.; Molnar, A.; Kiricsi, I. *Appl. Catal. A* **2002**, *232*, 67.

(27) Barrett, E. P.; Joyner, L. G.; Halenda, P. P. *J. Am. Chem. Soc.* **1951**, *73*, 373.
(28) Dutoit, D. C. M.; Schneider, M.; Hutter, R.; Baiker, A. *J. Catal.* **1996**, *161*, 651.
(29) Ren, J.; Li, Z.; Liu, S.; Xing, Y.; Xie, K. *Catal. Lett.* **2008**, *124*, 185.
(30) Prasad, M. R.; Madhavi, G.; Rao, A. R.; Kulkarni, S. J.; Raghavan, K. V. *J. Porous Mater.* **2006**, *13*, 81.
(31) Laha, S. C.; Kumar, R. *Microporous Mesoporous Mater.* **2002**, *53*, 163.
(32) Chen, W. H.; Ko, H. H.; Sakthivel, A.; Huang, S. J.; Liu, S. H.; Lo, A. Y.; Tsai, T. C.; Liu, S. B. *Catal. Today* **2006**, *116*, 111.
(33) Layman, K. A.; Ivey, M. M.; Hemminger, J. C. *J. Phys. Chem. B* **2003**, *107*, 8538.
(34) Rajagopal, S.; Marzari, J. A.; Miranda, R. *J. Catal.* **1995**, *151*, 192.
(35) Bordiga, S.; Coluccia, S.; Lamberti, C.; Marchese, L.; Zecchina, A.; Boscherini, F.; Buffa, F.; Genoni, F.; Leofanti, G. *J. Phys. Chem.* **1994**, *98*, 4125.
(36) Ricchiardi, G.; Damin, A.; Bordiga, S.; Lamberti, C.; Spano, G.; Rivetti, F.; Zecchina, A. *J. Am. Chem. Soc.* **2001**, *123*, 11409.
(37) Chen, Y. Y.; Huang, Y. L.; Xiu, J. H.; Han, X. W.; Bao, X. H. *Appl. Catal. A* **2004**, *273*, 185.
(38) Melero, J. A.; Arsuaga, J. M.; Frutos, P. d.; Iglesias, J.; Sainz, J.; Blázquez, S. *Microporous Mesoporous Mater.* **2005**, *86*, 364.
(39) Cagnoli, M. V.; Casuscelli, S. G.; Alvarez, A. M.; Bengoa, J. F.; Gallegos, N. G.; Samaniego, N. M.; Crivello, M. E.; Ghione, G. E.; Perez, C. F.; Herrero, E. R.; Marchetti, S. G. *Appl. Catal. A* **2005**, *287*, 227.
(40) Blasco, T.; Corma, A.; Navarro, M. T.; Pariente, J. P. *J. Catal.* **1995**, *156*, 65.
(41) Kuroki, M.; Asefa, T.; Whitnal, W.; Kruk, M.; Yoshina-Ishii, C.; Jaroniec, M.; Ozin, G. A. *J. Am. Chem. Soc.* **2002**, *124*, 13886.
(42) Namba, S.; Mochizuki, A. *Res. Chem. Intermed.* **1998**, *24*, 561.
(43) Wang, G. J.; Liu, G. Q.; Xu, M. X.; Yang, Z. X.; Liu, Z. W.; Liu, Y. W.; Chen, S. F.; Wang, L. *Appl. Surf. Sci.* **2008**, *255*, 2632.
(44) Díaz, I.; Pérez-Pariente, J. *Chem. Mater.* **2002**, *14*, 4641.
(45) Pauly, T. R.; Liu, Y.; Pinnavaia, T. J.; Billinge, S. J. L.; Rieker, T. P. *J. Am. Chem. Soc.* **1999**, *121*, 8835.
(46) Chao, M. C.; Lin, H. P.; Mou, C. Y.; Cheng, B. W.; Cheng, C. F. *Catal. Today* **2004**, *97*, 81.
(47) Eimer, G. A.; Chanquia, C. M.; Sapag, K.; Herrero, E. R. *Microporous Mesoporous Mater.* **2008**, *116*, 670.
(48) Gong, J. L.; Ma, X. B.; Wang, S. P. *Appl. Catal., A* **2007**, *316*, 1.
(49) Wang, S. P.; Ma, X. B.; Guo, H. L.; Gong, J. L.; Yang, X.; Xu, G. H. *J. Mol. Catal. A: Chem.* **2004**, *214*, 273.
(50) Ma, X. B.; Guo, H. L.; Wang, S. P.; Sun, Y. L. *Fuel Process. Technol.* **2003**, *83*, 275.
(51) Shi, Y.; Wang, S.; Ma, X. *Chem. Eng. J.* **2011**, *166*, 744.